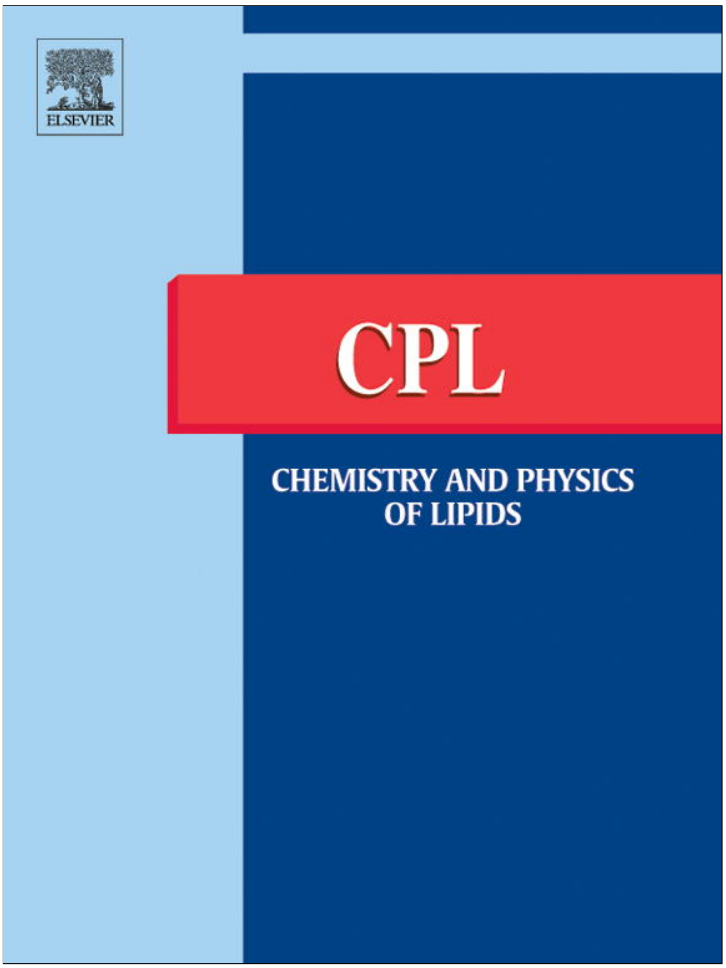

(This is a sample cover image for this issue. The actual cover is not yet available at this time.)

Chemistry and Physics of Lipids 165 (2012) 589–600

Contents lists available at SciVerse ScienceDirect

Chemistry and Physics of Lipids

journal homepage: www.elsevier.com/locate/chemphyslip

Structural effect of cationic amphiphiles in diacetylenic photopolymerizable membranes

C. Facundo Temprana[a,1,2], Evandro L. Duarte[b,1], A. Lis Femia[a,c], Silvia del V. Alonso[a,c], M. Teresa Lamy[b,*]

[a] Laboratorio de Biomembranas (LBM), Departamento de Ciencia y Tecnología, Universidad Nacional de Quilmes, Roque S. Peña 352, Bernal (B1876BXD), Buenos Aires, Argentina
[b] Instituto de Física, Universidade de São Paulo, CP 66318, CEP 05314-970, São Paulo, SP, Brazil
[c] IMBICE-CONICET, Calle 526 y Camino General Belgrano (entre 10 y 11) B1900BTE, La Plata, Buenos Aires, Argentina

ARTICLE INFO

Article history:
Received 18 April 2012
Received in revised form 15 June 2012
Accepted 19 June 2012
Available online xxx

Keywords:
Polymeric liposome
ESR
Spin label
DSC
Diacetylenic lipid
Cationic amphiphile

ABSTRACT

Liposomes have been an excellent option as drug delivery systems, since they are able of incorporating lipophobic and/or lipophilic drugs, reduce drug side effects, increase drug targeting, and control delivery. Also, in the last years, their use reached the field of gene therapy, as non-viral vectors for DNA delivery. As a strategy to increase system stability, the use of polymerizable phospholipids has been proposed in liposomal formulations. In this work, through differential scanning calorimetry (DSC) and electron spin resonance (ESR) of spin labels incorporated into the bilayers, we structurally characterize liposomes formed by a mixture of the polymerizable lipid diacetylenic phosphatidylcholine 1,2-bis(10,12-tricosadiynoyl)-sn-glycero-3-phosphocholine ($DC_{8,9}PC$) and the zwitterionic lipid 1,2-dimyristoyl-sn-glycero-3-phosphocholine (DMPC), in a 1:1 molar ratio. It is shown here that the polymerization efficiency of the mixture (c.a. 60%) is much higher than that of pure $DC_{8,9}PC$ bilayers (c.a. 20%). Cationic amphiphiles (CA) were added, in a final molar ratio of 1:1:0.2 ($DC_{8,9}PC$:DMPC:CA), to make the liposomes possible carriers for genetic material, due to their electrostatic interaction with negatively charged DNA. Three amphiphiles were tested, 1,2-dioleoyl-3-trimetylammonium-propane (DOTAP), stearylamine (SA) and trimetyl (2-miristoyloxietyl) ammonium chloride (MCL), and the systems were studied before and after UV irradiation. Interestingly, the presence of the cationic amphiphiles increased liposomes polymerization, MCL displaying the strongest effect. Considering the different structural effects the three cationic amphiphiles cause in $DC_{8,9}PC$ bilayers, there seem to be a correlation between the degree of $DC_{8,9}PC$ polymerization and the packing of the membrane at the temperature it is irradiated (gel phase). Moreover, at higher temperatures, in the bilayer fluid phase, more polymerized membranes are significantly more rigid. Considering that the structure and stability of liposomes at different temperatures can be crucial for DNA binding and delivery, we expect the study presented here contributes to the production of new carrier systems with potential applications in gene therapy.

1. Introduction

Liposomes have been widely used for many applications, from membrane models to drug delivery systems (Felnerova et al., 2004; Gregoriadis, 1995; Lundahl and Beigi, 1997; Samad et al., 2007; Sharma and Sharma, 1997; Ulrich, 2002). Different characteristics make liposomes an excellent option as a drug delivery system, such as the possibility to incorporate both lipophobic and lipophilic drugs, reduction of drug side effects, drug targeting, and controlled delivery (Felnerova et al., 2004; Gregoriadis, 1995; Kshirsagar et al., 2005; Moses et al., 2003; Mozafari, 2005; Poste et al., 1984; Rawat et al., 2008; Riaz, 1995; Sharma and Sharma, 1997). Moreover, in the last years, the use of liposomes has been proposed in gene therapy, as a non-viral vector system for DNA delivery (Elouahabi and Ruysschaert, 2005; Ishiwata et al., 2000; Rao, 2010; Tros de Ilarduya et al., 2010). No matter whether the

Abbreviations: DSC, differential scanning calorimetry; ESR, electron spin resonance; $DC_{8,9}PC$, 1,2-bis(10,12-tricosadiynoyl)-sn-glycero-3-phosphocholine; DMPC, 1,2-dimyristoyl-sn-glycero-3-phosphocholine; CA, cationic amphiphiles; DOTAP, 1,2-dioleoyl-3-trimetylammonium-propane; SA, stearylamine; MCL, trimetyl (2-miristoyloxietyl) ammonium chloride; 16-SASL, 16-doxyl-stearic acid; 16-PCSL, 1-palmitoyl-2-(16-doxylstearoyl)-sn-glycero-3- phosphocholine; τ_B or τ_C, rotational correlation times B or C; ΔH_0, linewidth of the central field line; ΔC_p, excess heat capacity; T_p, pre-transition temperature; T_m, transition temperature; $\Delta T_m^{1/2}$, half maximum width of the transition peak; ΔH_m, enthalpy variation; DPPC, 1,2-dipalmitoyl-sn-glycero-3-phosphocholine; POPC, 1-palmitoyl-2-oleoyl-sn-glycero-3-phosphocholine.

* Corresponding author. Tel.: +55 11 3091 6829; fax: +54 11 3813 4334.
E-mail address: mtlamy@if.usp.br (M.T. Lamy).
[1] Both authors contributed equally to this work.
[2] Present address: Laboratorio de Inmunología y Virología (LIV), Departamento de Ciencia y Tecnología, Universidad Nacional de Quilmes, Roque S. Peña 352, Bernal (B1876BXD), Buenos Aires, Argentina.

0009-3084/$ – see front matter © 2012 Elsevier Ireland Ltd. All rights reserved.
http://dx.doi.org/10.1016/j.chemphyslip.2012.06.007

carried substance is a drug or DNA, the stability of the system, *in vitro* and *in vivo*, has always been an important issue to be studied and improved (Alonso-Romanowski et al., 2003; Fabani et al., 2002; Gadras et al., 1999; Mohammed et al., 2004; Noble et al., 2009; Pouton and Seymour, 2001; Takeuchi et al., 1998; Tros de Ilarduya et al., 2010).

In the last decades, polymeric lipids have been studied as an option to increase liposome stability. When they are incorporated in lipid formulations, depending on the type of polymerizable lipid, intra and/or intermolecular covalent bonds between polar head groups or hydrophobic chains are generated after irradiation, improving membrane integrity in carrier systems, or planar supported lipid bilayers, among other systems (Ahl et al., 1990; Alonso-Romanowski et al., 2003; Blume, 1991; Clark et al., 2001; Daly et al., 2006; Freeman et al., 1987; Guo et al., 2010; Hayward et al., 1985; Markowitz et al., 1994; Morigaki et al., 2007; Subramaniam et al., 2008). In particular, it was shown that polymerized liposomes made of (1,2-bis(10,12-tricosadiynoyl)-sn-glycero-3-phosphocholine) ($DC_{8,9}PC$) and 1,2-dimyristoyl-sn-glycero-3-phosphocholine (DMPC) have a higher stability in different media when compared to the same non-polymerized formulation (Alonso-Romanowski et al., 2003). More recently, it was shown that the polymerization of $DC_{8,9}PC$:DMPC (1:1) liposome enhances time-storage stability, with no effect on the overall formulation toxicity (Temprana et al., 2011).

Considering that stability is a key issue in the design of new delivery systems, including those carrying DNA, the use of the $DC_{8,9}PC$:DMPC mixture (1:1, molar ratio) in the preparation of stable polymeric liposomes able to protect DNA from enzymatic degradation was proposed (Temprana, 2011). As liposome/DNA interaction is mainly governed by electrostatic forces (Elouahabi and Ruysschaert, 2005; Mel'nikova et al., 1999; Tros de Ilarduya et al., 2010; Zhang et al., 2003), a net positive charge was added to the liposome formulation, by the intercalation of cationic amphiphiles (CA), allowing the liposomes to spontaneously interact with DNA. Three different CA were used, namely 1,2-dioleoyl-3-trimetylammonium-propane (DOTAP), stearylamine (SA) and trimetyl (2-miristoyloxietyl) ammonium chloride (MCL), in a final 1:1:0.2 ($DC_{8,9}PC$:DMPC:CA) molar ratio. It was shown that the three systems interact with DNA, but the efficiency of the interaction was found to be lipid composition dependent, suggesting differences in their structural arrangement. Having in mind that the relationship between the structure of the liposome-DNA system and its biological function is a breaking point for a rational and systematic approach to the design of new carriers (Campbell et al., 2001a), the present work carefully investigates the structure of $DC_{8,9}PC$:DMPC:CA liposomes.

In a previous work, we structurally characterized the $DC_{8,9}PC$:DMPC mixture, finding the coexistence of rich domains of each lipid, when both $DC_{8,9}PC$ and DMPC are in the gel phase. After polymerization, these domains are maintained, though another component is present in the membrane: the polymeric units (Temprana et al., 2010). Here, we report our investigations on the thermo-structural behavior of $DC_{8,9}PC$:DMPC:DOTAP, $DC_{8,9}PC$:DMPC:SA and $DC_{8,9}PC$:DMPC:MCL, in a 1:1:0.2 molar ratio, before and after irradiation. Differential scanning calorimetry (DSC) was used to monitor bilayer thermal events, like the gel–fluid transition, which is extremely sensitive to lipid–lipid interaction and packing (see, for instance, Heimburg, 2000). Complementary to DSC, electron spin resonance (ESR) of spin labels incorporated into the lipid bilayers was used to provide independent information about membrane structural parameters (see, for instance, Marsh, 1990).

2. Materials and methods

2.1. Materials

The phospholipids 1,2-bis(10,12-tricosadiynoyl)-sn-glycero-3-phosphocholine ($DC_{8,9}PC$) and 1,2-dimyristoyl-sn-glycero-3-phosphocholine (DMPC) were purchased from Avanti Polar Lipids Inc. (Alabaster, AL, USA). Cationic amphiphiles (CA) 1,2-dioleoyl-3-trimetylammonium-propane (DOTAP) chloride and trimetyl (2-miristoyloxietyl) ammonium chloride (MCL) were from Toronto Research Chemicals Inc. (Toronto, Canada), and stearylamine (SA) was from Fluka-Riedel-de Haën (Seelze, Germany). The spin label 16-doxyl-stearic acid (16-SASL) was purchased from Sigma Chemical Co. (St. Louis, MO, USA) (all shown in Scheme 1). Lipids were used without further purification. All other reagents were of analytical grade and used without further purification. Milli-Q water was used throughout.

2.2. Liposome preparation

Liposomes were prepared as previously described (Temprana et al., 2010; Bangham et al., 1965). Briefly, 40 μmol total lipids were dissolved in chloroform and the solvent was removed under vacuum and flashed with nitrogen to obtain the lipid film. The saturated DMPC, or the polymerizable lipid $DC_{8,9}PC$, were mixed with the three different CA (DOTAP, SA, MCL) in a molar ratio DMPC or $DC_{8,9}PC$:CA (1:0.2). They were also mixed in a 1:1 molar ratio ($DC_{8,9}PC$:DMPC) in the absence and presence of the CA, in a 1:1:0.2 molar ratio ($DC_{8,9}PC$:DMPC:CA). These samples were suspended in distilled water to obtain a 5 mM total lipid concentration. Large unilamellar vesicles were obtained using a Mini Extruder from Avanti Polar Lipids Inc. (Alabaster, AL, USA) with a 200 nm membrane pore.

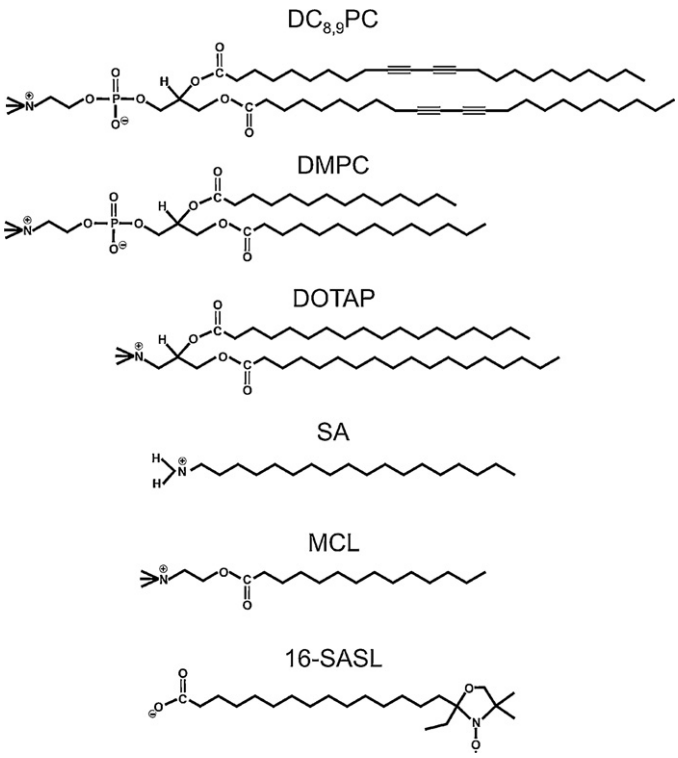

Scheme 1. Chemical structure of the phospholipids ($DC_{8,9}PC$ and DMPC), the cationic amphiphiles (DOTAP, SA and MCL), and the spin label (16-SASL) used here.

A Stratalinker UV Crosslinker 1800 lamp (Stratagene, La Jolla, CA, USA) for cross-linking was used to irradiate the lipid samples in order to induce the diacetylenic extruded vesicles polymerization. For each irradiation cycle, a 254 nm UV light dose of 360 mJ/cm^2 was used during 71 s per cycle. In order to improve the polymerization efficiency obtained in previous work (Temprana et al., 2010), lipids dispersions were prepared, as stated above, with a 5 mM total lipid concentration, instead of 10 mM used before, and the irradiated surface area was increased from 0.5 cm^2/mL to 2.0 cm^2/mL. Lipid dispersions underwent 20 irradiation cycles, maintaining the temperature at 4 °C for 5 min in between cycles. The absence of absorbance at $\lambda \sim 610$ nm ensured that there were vesicles and not tubules present in the suspension (Svenson and Messersmith, 1999; Alonso-Romanowski et al., 2003).

Samples were freeze-dried overnight under reduced pressure (in the range of 33×10^{-3} to 65×10^{-3} mbar) in a LABCONCO lyophilizer (Kansas City, MO, USA) and stored at −20 °C until further used.

For DSC and ESR measurements, freeze-dried samples were rehydrated adding 10 mM PBS buffer, pH 7.4, up to total lipid concentration of 10 mM.

For ESR measurements, lipid dispersions were added to dried films of 16-SASL (0.6 mol % of the total lipid concentration), heated up to 50 °C and vortexed for 5 min, so spin labels would incorporate into the lipid bilayers.

2.3. Differential scanning calorimetry (DSC)

DSC data were obtained with a Microcalorimeter (Microcal VP-DSC, Northampton, MA, USA). Temperature was varied from 5 up to 55 °C, at a scan rate of 20 °C/h or slower, at 5 °C/h, necessary for the ternary samples ($DC_{8,9}$PC:DMPC:CA). Total lipid concentration was 10 mM for all samples. Baseline subtractions and peak integrals were done with the MicroCal Origin software provided by MicroCal, as described before (Riske et al., 2009). All DSC data were obtained in triplicate. Very similar scans were obtained from different preparations for each dispersion, and identical profiles were obtained for the first, second and third scans of the same sample, so DSC scans shown here are highly reproducible, and were obtained from samples in thermal equilibrium. In Tables 1 and 2, numerical values are means, and uncertainties are standard deviations.

2.4. Electron spin resonance (ESR) spectroscopy

ESR measurements at X band were performed with an EMX spectrometer (Bruker, Germany). The sample temperature was controlled within 0.1 °C by a Bruker BVT-2000 variable temperature device, and varied from 5 to 60 °C. To ensure thermal equilibrium, before each scan the sample was left at the desired temperature for at least 10 min. ESR data were acquired immediately after sample preparation. Field-modulation amplitude of 1 G and microwave power of 10 mW were used.

All data shown are means of at least three experiments, and the uncertainties are the standard deviations. When not shown, uncertainties were found to be smaller than the size of the symbols.

In this work, the spin probe 16-SASL was used. The phospholipid spin probe 1-palmitoyl-2-(16-doxylstearoyl)-sn-glycero-3-phosphocholine (16-PCSL) could not be incorporated into $DC_{8,9}$PC membranes (Temprana et al., 2010).

For lipids in the gel phase, at low temperatures, the best parameter to be used is the direct measurement of the linewidth of the central field line, ΔH_0. This parameter is highly sensitive to chain order/mobility (Riske et al., 2009). At higher temperatures (45–70 °C), at the lipid fluid phase, the spin probe has a nearly

Table 1
Thermal parameters calculated from scans shown in Fig. 1, relative to DMPC (1) and $DC_{8,9}$PC (2) transitions, without and with the cationic amphiphiles DOTAP, SA and MCL: transition temperatures (T_{m1} and T_{m2}), half maximum width of the transition peaks ($\Delta T_{m1}^{1/2}$, $\Delta T_{m2}^{1/2}$) and enthalpy variations (ΔH_{m1} and ΔH_{m2}).

Sample	T_{m1} (°C)	$\Delta T_{m1}^{1/2}$ (°C)	ΔH_{m1} (kcal/mol of DMPC)	T_{m2} (°C)	$\Delta T_{m2}^{1/2}$ (°C)	ΔH_{m2} (kcal/mol of $DC_{8,9}$PC)
DMPC non-irradiated	23.9 ± 0.1	0.3 ± 0.1	5 ± 1			
DMPC irradiated	23.9 ± 0.2	0.3 ± 0.1	5 ± 1			
$DC_{8,9}$PC non-irradiated				44.0 ± 0.3	0.4 ± 0.1	21 ± 1
$DC_{8,9}$PC irradiated				43.2 ± 0.3	1.2 ± 0.1	17 ± 2 (81%)[a]
DMPC:DOTAP (1:0.2) non-irradiated	18.1 ± 0.3	7.1 ± 0.1	5.3 ± 0.2			
DMPC:DOTAP (1:0.2) irradiated	18.5 ± 0.1	6.5 ± 0.5	5 ± 1			
DMPC:SA (1:0.2) non-irradiated	–	–	6.2 ± 0.1			
DMPC:SA (1:0.2) irradiated	–	–	7.1 ± 0.6			
DMPC:MCL (1:0.2) non-irradiated	26.0 ± 0.1	0.4 ± 0.1	7.2 ± 0.1			
DMPC:MCL (1:0.2) irradiated	26.0 ± 0.1	0.5 ± 0.1	7.2 ± 0.4			
$DC_{8,9}$PC:DOTAP (1:0.2) non-irradiated				40.4 ± 0.1	2.7 ± 0.1	20 ± 2
$DC_{8,9}$PC:DOTAP (1:0.2) irradiated				39.4 ± 0.2	4.9 ± 0.1	15 ± 1 (73%)[a]
$DC_{8,9}$PC:SA (1:0.2) non-irradiated				–	–	23 ± 1
$DC_{8,9}$PC:SA (1:0.2) irradiated				–	–	12 ± 1 [(0)] (52%)[a]
$DC_{8,9}$PC:MCL (1:0.2) non-irradiated				42.3 ± 0.1	1.7 ± 0.1	18 ± 1
$DC_{8,9}$PC:MCL (1:0.2) irradiated				39.9 ± 0.1	4.8 ± 0.1	14.9 ± 0.2 (83%)[a]

[a] Percentage relative to the non-irradiated sample.

Table 2
Thermal parameters calculated from scans shown in Fig. 2, relative to the mixtures $DC_{8,9}PC$:DMPC, without and with the cationic amphiphiles DOTAP, SA and MCL: transition temperatures (T_{m1} and T_{m2}), half maximum width of the transition peaks ($\Delta T_{m1}^{1/2}$, $\Delta T_{m2}^{1/2}$) and enthalpy variations (ΔH_{m1} and ΔH_{m2}).

Sample	T_{m1} (°C)	$\Delta T_{m1}^{1/2}$ (°C)	ΔH_{m1} (kcal/mol of DMPC)	ΔH_m (kcal/mol of DMPC + $DC_{8,9}PC$)	T_{m2} (°C)	$\Delta T_{m2}^{1/2}$ (°C)	ΔH_{m2} (kcal/mol of $DC_{8,9}PC$)
DMPC:$DC_{8,9}PC$ (1:1) non-irradiated	23.1 ± 0.5	1.3 ± 0.3	5 ± 1		39.6 ± 0.4 (broad band)	3.4 ± 0.4	22 ± 1
DMPC:$DC_{8,9}PC$ (1:1) irradiated	25.2 ± 0.7	2.9 ± 0.5	7 ± 1				9 ± 1 (41%)[a]
DMPC:$DC_{8,9}PC$:DOTAP (1:1:0.2) non-irradiated	17.4 ± 0.2	5.2 ± 0.3	2.6 ± 0.4		37.8 ± 0.1 (broad band)	3.8 ± 0.2	22 ± 2
DMPC:$DC_{8,9}PC$:DOTAP (1:1:0.2) irradiated	23.0 ± 0.5	8.0 ± 1.0	5.0 ± 0.6				4.0 ± 1.5 (25%)[a]
DMPC:$DC_{8,9}PC$:SA (1:1:0.2) non-irradiated	–	–		15.9 ± 0.5[b]	–	–	
DMPC:$DC_{8,9}PC$:SA (1:1:0.2) irradiated	–	–		9 ± 1[b] (57%)[a]	–	–	
DMPC:$DC_{8,9}PC$:MCL (1:1:0.2) non-irradiated	24.4 ± 0.1	1.0 ± 0.1	8.2 ± 0.2		38.4 ± 0.1 (broad band)	3.5 ± 0.1	24.4 ± 0.2
DMPC:$DC_{8,9}PC$:MCL (1:1:0.2) irradiated	25.6 ± 0.1	6.7 ± 0.1	9.0 ± 0.2				3.9 ± 0.2 (16%)[a]

T_{m1}, $\Delta T_{m1}^{1/2}$ and ΔH_{m1} refer to DMPC or DMPC rich regions, and ΔH_{m2}, $\Delta T_{m2}^{1/2}$ and ΔT_{m2} refer to $DC_{8,9}PC$ or $DC_{8,9}PC$ rich regions.
[a] Percentage relative to the non-irradiated sample ($DC_{8,9}PC$ monomers).
[b] As it is not possible to separately distinguish DMPC and $DC_{8,9}PC$ transitions (see Fig. 2), the normalized lipid concentration was [DMPC] + [$DC_{8,9}PC$].

isotropic movement, and rotational correlation times can be calculated from the peak-to-peak width of the ESR Lorentzian lines, according to the motional narrowing theory (Freed and Fraenkel, 1963; Hubbell and McConnell, 1971; Schreier et al., 1978):

$$\Delta H_L(m) = A + Bm + Cm^2$$

where m is the mth component of the nitrogen nuclear spin ($m = 0$, 1 or −1), A is the Lorentzian linewidth of the central line ($\Delta H_L(0)$), and B and C are

$$B = \frac{1}{2}\Delta H_L(0)\left(\frac{\Delta H_L(+1)}{\Delta H_L(0)} - \frac{\Delta H_L(-1)}{\Delta H_L(0)}\right)$$

$$C = \frac{1}{2}\Delta H_L(0)\left(\frac{\Delta H_L(+1)}{\Delta H_L(0)} + \frac{\Delta H_L(-1)}{\Delta H_L(0)} - 2\right)$$

The correlation time for doxyl labels is either $\tau_B = -1.22$ ns B or $\tau_C = 1.19$ ns C, ($\tau_B = \tau_C$ for isotropic movement). Lorentzian linewidths are calculated using a computer program, which performs nonlinear least-square fitting of the experimental ESR spectrum using a model of a Lorentzian–Gaussian function for corrections for non-resolved hyperfine splitting (Halpern et al., 1993; Bales, 1989).

3. Results and discussion

Though the focus of this work is the structural study of ternary bilayers, $DC_{8,9}PC$:DMPC:CA (1:1:0.2), we found that the knowledge of the effect cationic amphiphiles cause on DMPC and $DC_{8,9}PC$ bilayers, separately, was fundamental to the understanding of their effect on the mixture, $DC_{8,9}PC$:DMPC. Hence, with both DSC and ESR, the study with binary mixtures of DMPC:CA (1:0.2) and $DC_{8,9}PC$:CA (1:0.2) is discussed before the analysis of the effects caused by cationic amphiphiles on the more complex system, $DC_{8,9}PC$:DMPC.

3.1. DSC

Fig. 1 shows DSC scans of non-irradiated and irradiated dispersions of pure DMPC and $DC_{8,9}PC$, and dispersions of each phospholipid mixed with the cationic amphiphiles DOTAP, SA and MCL (see Section 2.2).

As expected, and previously reported by Temprana et al. (2010), the DSC profile of DMPC (Marsh, 1990) does not change upon irradiation, presenting a pre-transition around 15 °C (indicated as T_p in Fig. 1, at 15.0 °C), and a main gel–fluid transition at 23.9 °C. For $DC_{8,9}PC$, after irradiation, which is known to cause lipid polymerization (Alonso-Romanowski et al., 2003; Temprana et al., 2010), the membrane transition temperature does not change much, but the transition was found to be less cooperative ($\Delta T_{m2}^{1/2}$ increases from 0.4 to 1.2 °C, see Table 1). The gel–fluid transition enthalpy varied from 21 ± 1 to 17 ± 2 kcal/mol, after irradiation, hence approximately decreasing to 81% of its original value (Table 1). It is important to have in mind that in polymerized lipids the phase transition is completely eliminated, as chains are extensively cross-linked (Blume, 1991; Hayward et al., 1985). Hence, as the measured enthalpy variation is due to non-polymerized units only, it can be concluded that even with the new polymerization methodology used here (see Section 2.2), only a small percentage of lipids were polymerized, less than 20% of $DC_{8,9}PC$ monomers (since even non-polymerized lipids at the edges of $DC_{8,9}PC$ polymerized domains are not expected to contribute to the gel–fluid transition enthalpy). Therefore, as discussed in Temprana et al. (2010), in $DC_{8,9}PC$ UV irradiated bilayers there is a coexistence of large non polymerized lipid regions with small polymerized domains.

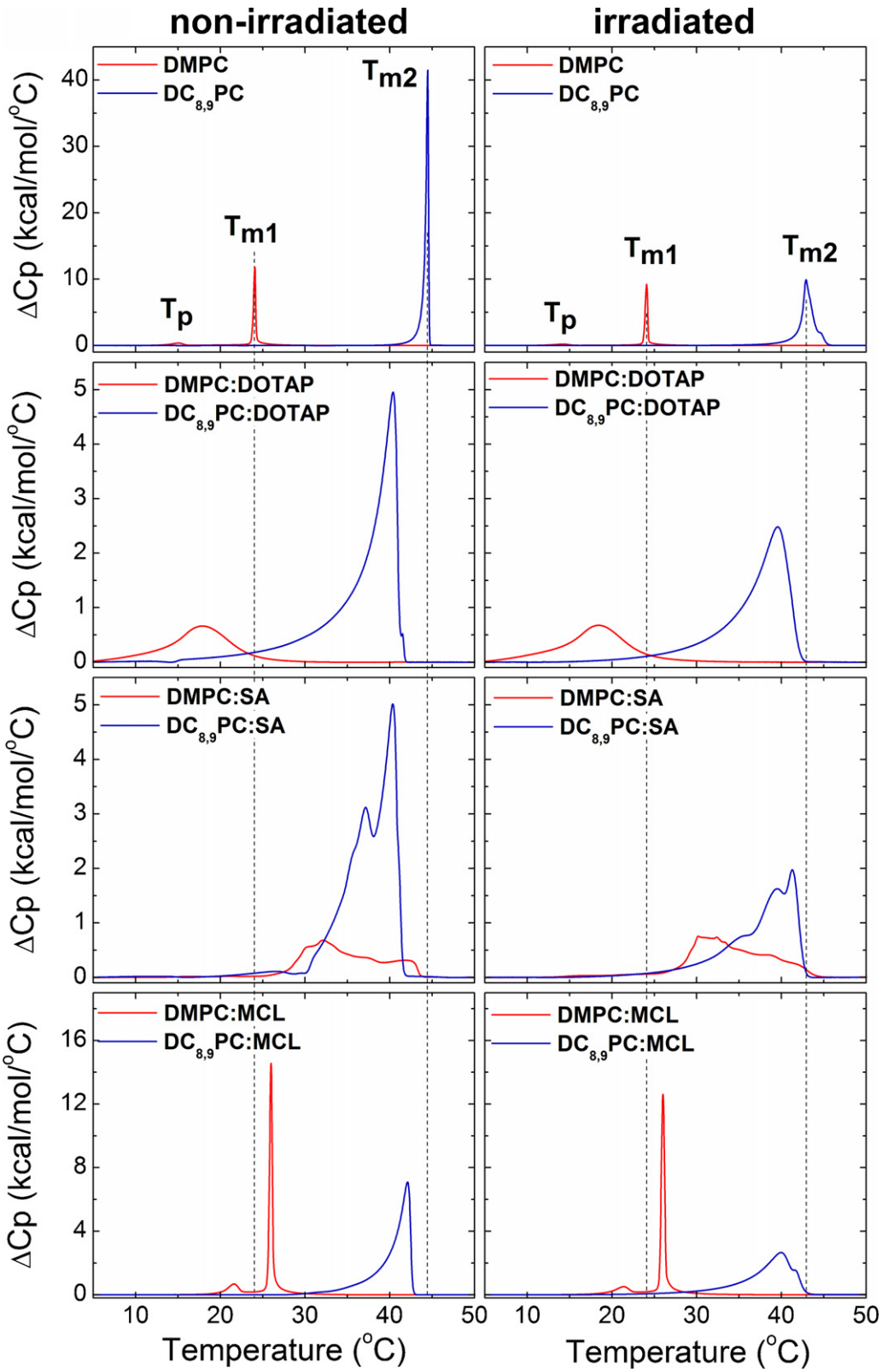

Fig. 1. Typical excess heat capacity (ΔC_p) profiles of DMPC and $DC_{8,9}PC$, non-irradiated and irradiated (left and right column, respectively), pure (top scans), and with 0.2 mol% of DOTAP, SA and MCL (as indicated in the figure). Dashed lines are just for guiding the eyes.

The presence of 20 mol% of cationic amphiphile significantly changes the phospholipids gel–fluid transition, but it is interesting to see that DOTAP, SA and MCL cause distinct effects on the bilayers (Fig. 1). The double chain DOTAP broadens the transition of both DMPC and $DC_{8,9}PC$, and decreases the transition temperatures. Hence, DOTAP destabilizes the gel phases of DMPC and $DC_{8,9}PC$, strongly reducing the gel–fluid transition cooperativity. This fluidizing effect of DOTAP, and loss of cooperativity in a gel lipid bilayer, has been observed before, by fluorescence polarization, with membranes of DPPC (1,2-dipalmitoyl-sn-glycero-3-phosphocholine) and DMPC with DOTAP (Campbell et al., 2001a,b). More specifically, a gradual decrease in the gel–fluid transition temperature of the phosphatidylcholines was observed with increasing concentrations of DOTAP, starting at very low DOTAP concentrations (0.4 mol%). The studies reported by Campbell et al., 2001a,b, suggested that the two DOTAP acyl chains penetrate DMPC bilayers, and that both lipids are miscible at all proportions studied (Campbell et al., 2001a), forming stable vesicles at physiological temperature.

As expected, upon irradiation, the DSC trace of DMPC:DOTAP liposomes does not change (Fig. 1, Table 1). For $DC_{8,9}PC$:DOTAP bilayer, the gel–fluid transition becomes broader, and the transition enthalpy decreases to 73% of its original value (before irradiation), as compared with 81% without DOTAP (Table 1), hence the percentage of polymerized lipids seems to increase. Considering that the irradiation process is performed at low temperatures (see Section 2.2), it is curious to observe that the disordering effect caused by DOTAP on $DC_{8,9}PC$ bilayers increases the bilayer polymerization efficiency. That will be better discussed in the next section, together with ESR results obtained with the three cationic amphiphiles incorporated in $DC_{8,9}PC$ bilayers.

The effect of SA on the DMPC transition is drastic: it shifts the transition to much higher values, hence, apparently, stabilizing the gel phase of DMPC. But SA significantly broadens the gel–fluid transition (Fig. 1), hence decreases lipid cooperativity. Actually, the change from a DMPC:SA more ordered to a less ordered bilayer seems to be a process consisting of several thermal events. Opposite to that, the effect caused by SA on $DC_{8,9}PC$ is to decrease the gel–fluid transition temperature, but it also causes a split on the transition, giving rise to several peaks on the DSC scan (due to the presence of several thermal events, Table 1 does not include T_m or ΔT_m values for DMPC:SA and $DC_{8,9}PC$:SA dispersions). Irradiation does not change much the DSC profile of $DC_{8,9}PC$:SA dispersion, but the transition enthalpy is significantly reduced to around 50% of its original value (Table 1). Hence, SA is the cationic amphiphile tested here most efficient in increasing $DC_{8,9}PC$ polymerization.

The effect of MCL on DMPC bilayers is noteworthy: T_{m1} is shifted to higher values (from 23.9 to 26.0 °C), $\Delta T_{m1}^{1/2}$ does not change much, and ΔH_{m1} increases from 5 to 7.2 kcal/mol (Fig. 1 and Table 1). Hence, the presence of MCL stabilizes the DMPC gel phase, even preserving the pre-transition, present at a higher temperature, T_p = 21.6 °C as compared with T_p = 15.0 °C, for pure DMPC samples (Fig. 1). Opposite to that, the effect of MCL on $DC_{8,9}PC$ bilayers is somehow similar to the effect of the other cationic amphiphiles, DOTAP and SA, decreasing the $DC_{8,9}PC$ gel–fluid transition temperature, and broadening the transition. Different from SA, MCL does not change much the percentage of $DC_{8,9}PC$ polymerization, keeping it around 20% (~83% of monomeric $DC_{8,9}PC$, in Table 1).

The left column of Fig. 2 displays DSC scans of non-irradiated dispersions of $DC_{8,9}PC$:DMPC, $DC_{8,9}PC$:DMPC:DOTAP, $DC_{8,9}PC$:DMPC:SA and $DC_{8,9}PC$:DMPC:MCL (for preparation, see Section 2.2). Fig. 2a corresponds to the DSC scan of non-irradiated mixture $DC_{8,9}PC$:DMPC, which is similar to that obtained before (Temprana et al., 2010). It is evident that the two phospholipids are partially mixed: both DMPC and $DC_{8,9}PC$ transitions are significantly broadened, and shifted to lower temperature values (to be compared with scans in Fig. 1), and DMPC and $DC_{8,9}PC$ rich regions can be identified by the two transition temperatures (1 and 2, respectively, in Table 2). Table 2 shows a tentative analysis of the two transitions separately, from DMPC and $DC_{8,9}PC$ rich domains, the first and second endothermic bands in DSC profiles (in Fig. 2, the $DC_{8,9}PC$ rich region transition is assigned, striped). As observed before for DMPC:SA dispersion (Fig. 1), SA shifts DMPC rich domain transition to much higher values (Fig. 2e), making impossible the distinction between the two transitions, from DMPC and $DC_{8,9}PC$ rich domains, hence, in Table 2, ΔH_m is the sum of $\Delta H_{m1} + \Delta H_{m2}$.

As mentioned above, the new polymerization methodology used here, with a 2-fold decrease in the lipid concentration, and a 4-fold increase in the irradiated surface area per volume, did not improve the polymerization efficiency of pure $DC_{8,9}PC$ bilayers, as compared with previous experiments (Temprana et al., 2010). However, a huge difference was observed with the mixture $DC_{8,9}PC$:DMPC, with the two polymerization procedures (the old and the new one). With the new procedure used here, a remarkable effect on the polymerization efficiency was obtained, together with significant changes on the transition profiles of both DMPC and $DC_{8,9}PC$ rich regions (Fig. 2b). Hence, the percentage of polymerized lipids increased from 20 to around 60%, with $DC_{8,9}PC$ mixed with DMPC (comparing Tables 1 and 2, for $DC_{8,9}PC$ and $DC_{8,9}PC$:DMPC samples, respectively).

To better analyze the effect of the three cationic amphiphiles on the DSC profile of the mixture $DC_{8,9}PC$:DMPC, theoretical additions of the scans obtained with the amphiphiles incorporated in pure DMPC and $DC_{8,9}PC$ vesicles (shown in Fig. 1) are displayed in Fig. 2 (gray lines). For non-irradiated samples (left column), the effect the cationic amphiphile causes on the bilayers, hence on the DSC scans of the mixture $DC_{8,9}PC$:DMPC:CA (black lines), is somewhat similar to the effect it causes on each lipid ($DC_{8,9}PC$ and DMPC) separately (gray lines). Hence, apparently, the presence of the cationic amphiphile does not alter much the balance of $DC_{8,9}PC$ and DMPC rich domains along the lipid bilayer, though some differences are observed between experimental DSC traces ($DC_{8,9}PC$:DMPC:CA) and theoretical additions ($DC_{8,9}PC$:CA + DMPC:CA), black and gray lines, respectively, in Fig. 2c, e and g. It is important to have in mind that the theoretical gray lines in Fig. 2 were obtained with the ratio phospholipid:CA, 1:0.2, and in the ternary samples the relation is $DC_{8,9}PC$:DMPC:CA, 1:1:0.2. So, gray lines correspond to the maximum possible effect caused by the CA in each domain ($DC_{8,9}PC$ or DMPC rich domain), considering that the CA would be totally partitioned in that area.

For irradiated samples of the mixture $DC_{8,9}PC$:DMPC, with cationic amphiphiles (Fig. 2d, f and h), DSC scans are very different from those obtained by the theoretical addition of irradiated $DC_{8,9}PC$:CA + DMPC:CA dispersions (gray lines). Considering the significant decrease in ΔH_{m2} caused by the presence of DOTAP and MCL in irradiated $DC_{8,9}PC$:DMPC:CA samples (25 and 16%, respectively, in Table 2), one can infer that these cationic amphiphiles are very effective in increasing the polymerization efficiency of irradiated $DC_{8,9}PC$.

3.2. ESR

The same dispersions studied by DSC ($DC_{8,9}PC$, DMPC and $DC_{8,9}PC$:DMPC, pure and with the three cationic amphiphiles, DOTAP, SA and MCL), non-irradiated and irradiated, were structurally analyzed *via* the ESR signal of a stearic acid spin labeled at the 16th carbon atom, 16-SASL, incorporated in the vesicles, at the gel and fluid phases of the bilayers. This spin probe was chosen because it is sensitive to bilayer packing and order, as it labels the

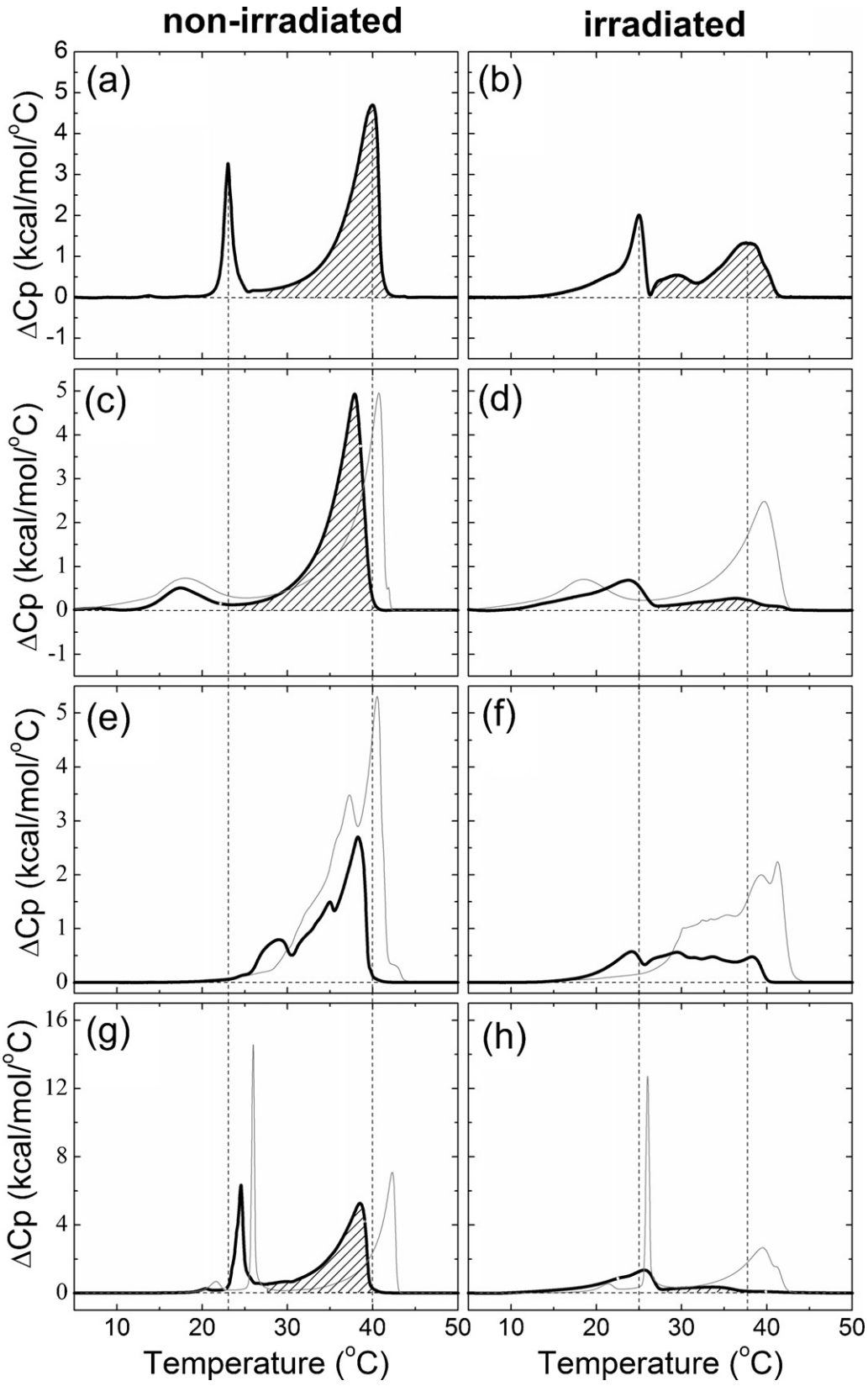

Fig. 2. Typical excess heat capacity (ΔC_p) profiles of the mixture $DC_{8,9}PC$:DMPC (1:1), non-irradiated (a, c, e and g) and irradiated (b, d, f and h), pure (a and b), and with 0.2 mol% of DOTAP (c and d), SA (e and f) and MCL (g and h). For comparison, the theoretical addition of the scans shown in Fig. 1, of pure DMPC and $DC_{8,9}PC$ with the cationic amphiphiles DOTAP (c and d), SA (e and f) and MCL (g and h) are also shown (gray lines). Dashed lines are just for guiding the eyes.

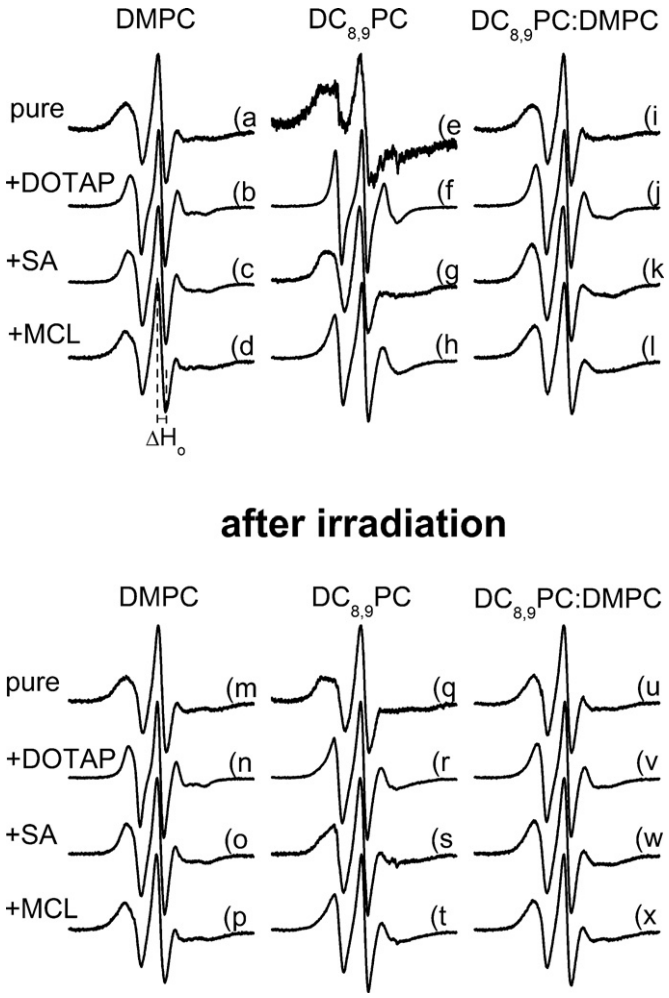

Fig. 3. ESR spectra of 16-SASL in non-irradiated and irradiated DMPC, $DC_{8,9}PC$ and $DC_{8,9}PC$:DMPC dispersions, in the absence and in the presence of DOTAP, SA and MCL (total lipid concentration 10 mM), at 5 °C (gel phase). Spectra are shown after subtracting the spectrum due to 16-SASL free in solution, as discussed in Temprana et al., 2010. Total spectra width 100 G. Spectra are normalized to the maximum signal amplitude.

bilayer core (Temprana et al., 2010; Benatti et al., 2001; Griffith and Jost, 1976).

Fig. 3 shows the ESR spectra of 16-SASL in dispersions of $DC_{8,9}PC$, DMPC and $DC_{8,9}PC$:DMPC, pure and with the three cationic amphiphiles, DOTAP, SA and MCL, non-irradiated (a to l, Fig. 3) and after UV irradiation (m to x, Fig. 3). Spectra were obtained at 5 °C, hence below the gel–fluid transition of the two phospholipids, for all samples studied (see DSC scans, Figs. 1 and 2). The shown ESR spectra are due to the label incorporated into the bilayers, as the signal due to spin label in solution was subtracted from the experimental spectra, as discussed before (Temprana et al., 2010).

Spectra of 16-SASL shown in Fig. 3 are rather anisotropic, typical of the spin label in gel bilayers (see, for instance, Hubbell and McConnell, 1971). As discussed before (Temprana et al., 2010), possibly due to the high packing of the $DC_{8,9}PC$ bilayer in the gel phase, either polymerized or not, spin labels do not seem to be uniformly distributed in the gel phase of this phospholipid, and ESR spectra (e and q, Fig. 3) appear to be distorted by spin–spin interaction (Jost and Griffith, 1976). Curiously, the ESR spectrum obtained with 16-SASL incorporated in $DC_{8,9}PC$ bilayers before irradiation (e), indicates stronger spin–spin interaction than that yielded after polymerization (q).

ESR signals yielded by 16-SASL in gel bilayers (Fig. 3) can be compared by analysing the central field linewidth, ΔH_0 (see spectrum d in Fig. 3), which gets smaller as the micro-environment monitored by the spin label gets less packed (Hubbell and McConnell, 1971). As expected, ΔH_0 decreases as temperature increases (Fig. 4).

In DMPC membranes (either before or after irradiation), considering the measured ΔH_0 values (Fig. 4a and b), both SA and MCL do not seem to significantly alter the bilayer packing at low temperatures (SA causes a small ΔH_0 decrease, but only at 5 °C). However, DOTAP makes DMPC gel bilayers less packed, considerably decreasing the anisotropy of the 16-SASL ESR spectrum (b and n, as compared to a and m, Fig. 3), and causing a significant decrease in ΔH_0 values (Fig. 4a and b). This is entirely in accord with the shift to lower temperatures and the broadening of the DMPC gel–fluid transition monitored by DSC, hence destabilizing the DMPC gel phase, only observed for the DMPC:DOTAP dispersion (Fig. 1). Though SA significantly broadens DMPC gel–fluid transition, it somehow stabilizes the gel phase, shifting the transition temperature to higher values (Fig. 1).

Though ΔH_0 values are not very reliable for $DC_{8,9}PC$ bilayers, due to spin–spin interaction (as discussed above), the three cationic amphiphiles seem to turn the $DC_{8,9}PC$ gel bilayer significantly more fluid, mainly for non-irradiated samples, decreasing the central field linewidth (Fig. 4c and d). Actually, ESR spectra of 16-SASL incorporated into $DC_{8,9}PC$ bilayers with DOTAP (f and r spectra, Fig. 3) and MCL (h and t spectra, Fig. 3) are clearly due to a label in a more fluid environment (more isotropic spectra; see for instance, Hubbell and McConnell, 1971) than when incorporated in pure $DC_{8,9}PC$ bilayers (e and q spectra, Fig. 3), before and after irradiation. Hence, spin labels seem to be homogenously distributed in the membrane and no spin–spin interaction is detected. A similar discussion is not so obvious considering the spectra yielded by 16-SASL in $DC_{8,9}PC$:SA bilayers (g and s spectra, Fig. 3). The fluidizing effect of the cationic amphiphiles in $DC_{8,9}PC$ gel bilayer is in accord with their effect in decreasing the $DC_{8,9}PC$ gel–fluid transition temperature and cooperativity, significantly increasing the transition width (see Fig. 1). Having in mind that the polymerization process is performed at low temperatures, it is interesting to observe that though DOTAP and SA increase the $DC_{8,9}PC$ gel-bilayer fluidity (decrease ΔH_0 values, Fig. 4c), somehow they facilitate the interaction among $DC_{8,9}PC$ diacetylenic groups, increasing bilayer polymerization (see Table 1). However, SA, the cationic amphiphile that causes the smallest decrease in ΔH_0 values of $DC_{8,9}PC$ bilayers before irradiation (Fig. 4c), hence on the gel bilayer packing, is the one that causes the highest increase in the degree of $DC_{8,9}PC$ polymerization upon irradiation, from around 20% ($DC_{8,9}PC$) to 50% ($DC_{8,9}PC$:SA) (Table 1).

For the mixture, $DC_{8,9}PC$:DMPC, before or after irradiation (spectra i and u, respectively, in Fig. 3) spin labels seem to be mostly incorporated in DMPC rich domains, as the ESR spectra are very similar to those yielded by 16-SASL in DMPC dispersions (spectra a and m, Fig. 3), which is confirmed by measured ΔH_0 values for DMPC and $DC_{8,9}PC$:DMPC samples (Fig. 4a, b, e and f). That is possibly due to the rigidity of gel $DC_{8,9}PC$ rich domains (Temprana et al., 2010), causing a better spin label partition in DMPC rich regions. Hence, for $DC_{8,9}PC$:DMPC liposomes in the gel phase, spin label seems to give structural information about DMPC rich domains only. However, for the ternary samples, $DC_{8,9}PC$:DMPC:CA (Fig. 3, spectra j, k, l, v, w and x), it is impossible to say how the spin label is distributed, as the cationic amphiphiles make the gel $DC_{8,9}PC$ bilayer more fluid, as discussed above, which could mean that the spin label is better partitioned among the different domains in the membrane. But similar to the effect observed with DMPC (Fig. 4a and b), DOTAP is the only cationic amphiphile that significantly decreases the fluidity of gel $DC_{8,9}PC$:DMPC bilayers, both non-irradiated and irradiated (decreases ΔH_0 values, Fig. 4e and f).

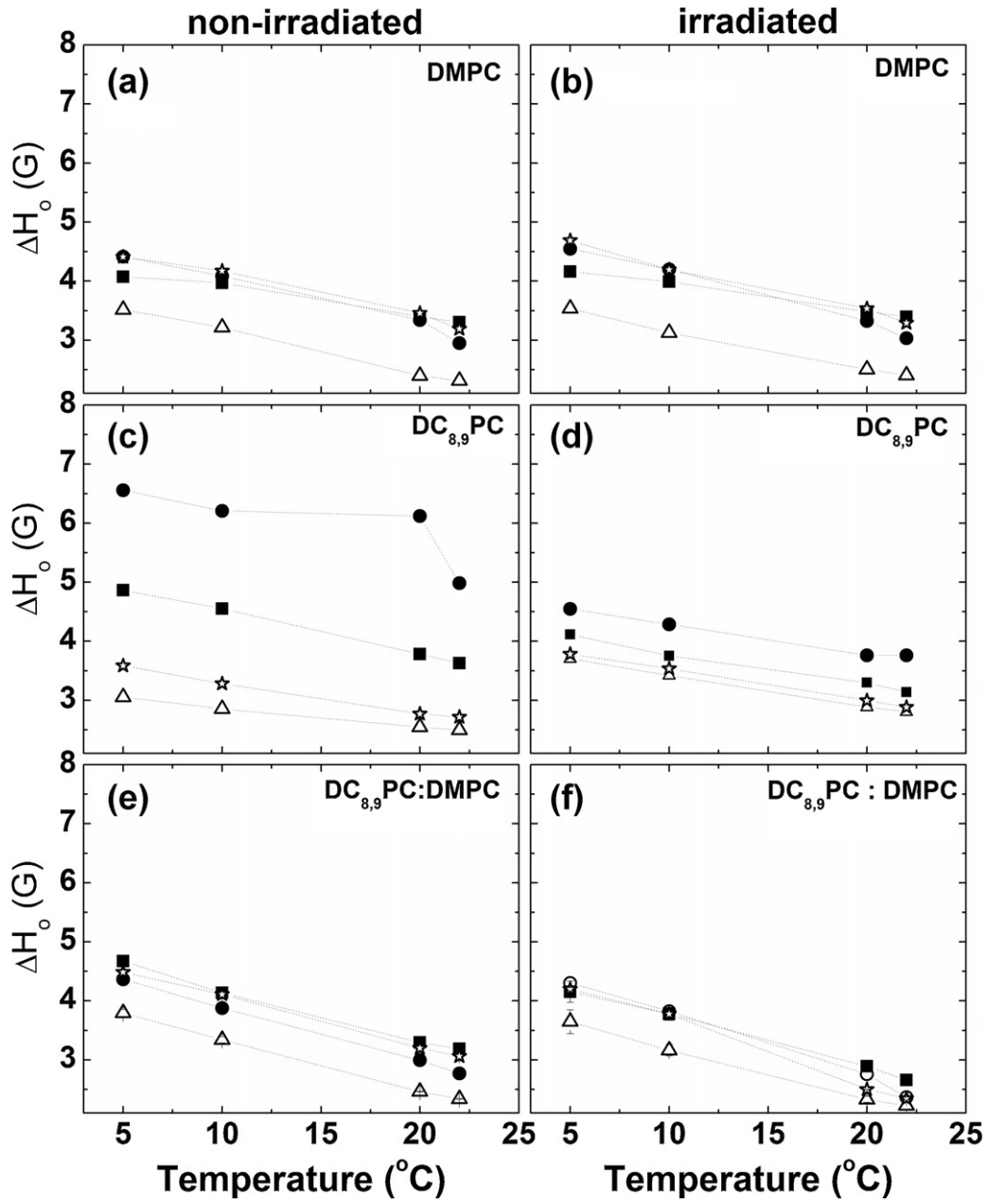

Fig. 4. Central field linewidth, ΔH_0 (see Fig. 3), directly measured on the ESR spectra of 16-SASL incorporated into non-irradiated (left column) and irradiated (right column) bilayers of DMPC, $DC_{8,9}PC$, and $DC_{8,9}PC$:DMPC, pure (●), and with the cationic amphiphiles DOTAP (△), SA (■) and MCL (☆), at low temperatures. When not shown, uncertainties are smaller than the size of the symbols.

For fluid membranes (above 45 °C), 16-SASL incorporated in DMPC, $DC_{8,9}PC$ and $DC_{8,9}PC$:DMPC liposomes, with and without the cationic amphiphiles, non-irradiated and irradiated, yield ESR spectra typical of spin labels in rather fluid and isotropic domains (three narrow peaks, typical of the motional narrowing regime, (see Fig. 9 in Temprana et al., 2010). Hence, membrane structure could be well analyzed by the rotational correlation time of 16-SASL incorporated into the bilayers. As discussed in Section 2, two rotational correlation times were calculated, τ_B and τ_C, and were found to be very similar for temperatures above 45 °C, indicating a nearly isotropic movement for the probe in these bilayers (Griffith and Jost, 1976). Hence, Fig. 5 shows values of τ_C obtained for all dispersions studied here, before and after irradiation. As expected, rotational correlation times decrease as temperature increases. As found before (Temprana et al., 2010), τ_C values yielded by spin labels incorporated in the mixture $DC_{8,9}PC$:DMPC were found to be in between values obtained with pure DMPC and $DC_{8,9}PC$, for both non-irradiated and irradiated dispersions (Fig. 5). Hence, either DMPC and $DC_{8,9}PC$ get mixed up when both lipids are in the fluid phase, irradiated or not, or spin labels move relative quickly between DMPC and $DC_{8,9}PC$ rich domains (compared to the microwave frequency used), yielding an average ESR signal.

Curiously, for non-irradiated samples at the fluid phase, MCL was the only cationic amphiphile to significantly change (fluidizes) bilayers of DMPC, $DC_{8,9}PC$ and $DC_{8,9}PC$:DMPC (decreases the label rotational correlation time, Fig. 5a, c and e). That is different from the result obtained with DOTAP in unsaturated bilayers of

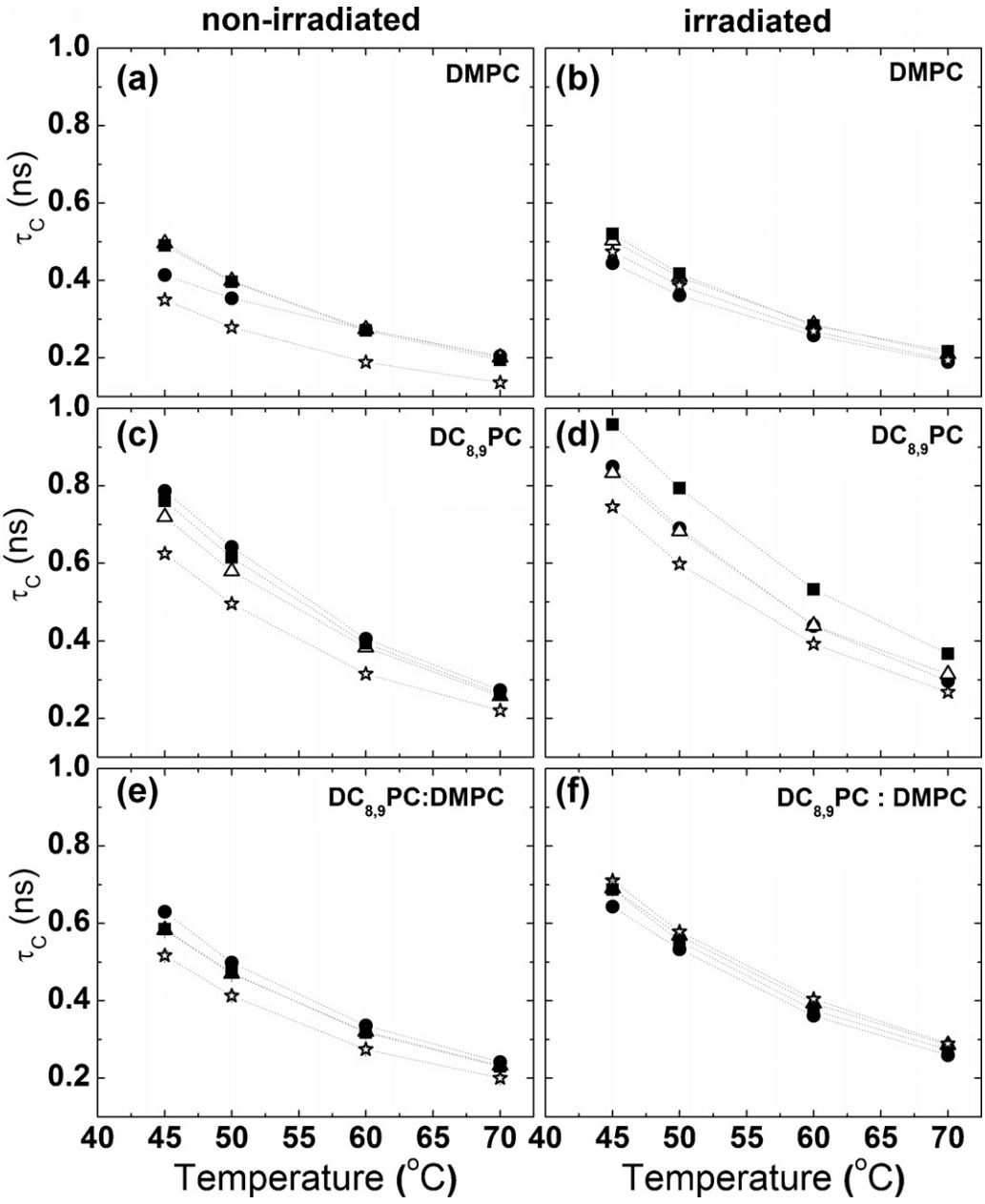

Fig. 5. Rotational correlation time (τ_C) of 16-SASL incorporated into non-irradiated (left column) and irradiated (right column) dispersions of DMPC, $DC_{8,9}PC$, and $DC_{8,9}PC$:DMPC, pure (●), and with the cationic amphiphiles DOTAP (△), SA (■) and MCL (☆), at high temperatures. When not shown, uncertainties are smaller than the size of the symbols.

POPC (1-palmitoyl-2-oleoyl-sn-glycero-3-phosphocholine), where 7 mol% was found to significantly decrease the bilayer fluidity (Benatti et al., 2008). Clearly, DMPC:MCL bilayers are less fluid after irradiation (larger τ_C values), though the rationale behind this finding is not clear. In general, for irradiated and polymerized samples ($DC_{8,9}PC$ and $DC_{8,9}PC$:DMPC, with or without CA), τ_C values increase (compare Fig. 5a,c, e with b, d, f, respectively). This effect is somehow expected, as the presence of polymerized units should increase the packing of a bilayer in the fluid phase. Interestingly, the great increase in polymerization caused by the presence of SA in $DC_{8,9}PC$ liposomes (compare ΔH_{m2} values in Table 1) is detected by ESR, as polymerized fluid bilayers of $DC_{8,9}PC$:SA are significantly more rigid than those of pure $DC_{8,9}PC$, or $DC_{8,9}PC$ with DOTAP or MCL (larger τ_C values in Fig. 5d). Moreover, for the mixture $DC_{8,9}PC$:DMPC, the great increase in polymerization caused by MCL (compare ΔH_{m2} values in Table 2) is also reflected in a higher packing for $DC_{8,9}PC$:DMPC:MCL fluid membranes (larger τ_C values in Fig. 5f).

4. Conclusions

In this work we studied the polymerization efficiency and the structural effect of cationic amphiphiles addition to $DC_{8,9}PC$:DMPC (1:1) membranes. With the new polymerization process used here, an improved polymerization efficiency of $DC_{8,9}PC$:DMPC membranes was obtained: from around 20% (Temprana et al., 2010) to c.a. 60%. Moreover, addition of MCL to the phospholipid mixture ($DC_{8,9}PC$:DMPC:MCL, 1:1:0.2) resulted in an even higher polymerization efficiency (c.a. 80%), followed by $DC_{8,9}PC$:DMPC:DOTAP (c.a. 75%) (Table 2). Due to a complex DSC profile, nothing can be said about the $DC_{8,9}PC$:DMPC:SA sample (Fig. 2 and Table 2).

By spin labels intercalated into the membrane (Fig. 4), DOTAP and MCL were found to disturb more the gel phase of $DC_{8,9}PC$ than SA (decrease ΔH_0 values). Curiously, the degree of $DC_{8,9}PC$ polymerization was found to be higher for $DC_{8,9}PC$:SA samples than for $DC_{8,9}PC$:DOTAP or $DC_{8,9}PC$:MCL (Table 1). Thus, there is a correlation between the degree of $DC_{8,9}PC$ polymerization and the packing of the membrane at the temperature it is irradiated. ESR of spin labels also correlated more polymerized membranes with more rigid bilayers in the fluid phase.

Small amount of polymeric $DC_{8,9}PC$ (c.a. 20%) was found to improve the system stability in different media (Alonso-Romanowski et al., 2003; Temprana et al., 2010). Addition of CA to $DC_{8,9}PC$:DMPC membranes not only allow DNA interaction (Temprana, 2011) but, as studied in this work, improve $DC_{8,9}PC$ polymerization (particularly MCL and DOTAP), and thus strongly contributes to the system stability, which is a key issue in delivery systems.

Considering that the structure and stability of liposomes at different temperatures are crucial for DNA binding and delivery, we expect the study presented here contributes to the production of new carrier systems with potential applications in gene therapy.

Acknowledgments

This work was supported by USP, FAPESP, CNPq (MTL and ELD research fellowships), UNQ, CONICET (SdelVA Research Career, CFT and ALF research fellowships) and MINCyT.

References

Ahl, P.L., Price, R., Smuda, J., Gaber, B.P., Singh, A., 1990. Insertion of bacteriorhodopsin into polymerized diacetylenic phosphatidylcholine bilayers. Biochimica et Biophysica Acta 1028, 141–153.

Alonso-Romanowski, S., Chiaramoni, N.S., Lioy, V.S., Gargini, R.A., Viera, L.I., Taira, M.C., 2003. Characterization of diacetylenic liposomes as carriers for oral vaccines. Chemistry and Physics of Lipids 122, 191–203.

Bales, B.L., 1989. Inhomogeneously broadened spin-label spectra. In: Berliner, L.J., Reuben, J. (Eds.), Biological Magnetic Resonance. Plenum Publishing Corporation, New York, pp. 77–130.

Bangham, A.D., Standish, M.M., Watkins, J.C., 1965. Diffusion of univalent ions across lamellae of swollen phospholipids. Journal of Molecular Biology 13, 238–252.

Benatti, C.R., Feitosa, E., Fernandez, R.M., Lamy-Freund, M.T., 2001. Structural and thermal characterization of dioctadecyldimethylammonium bromide dispersions by spin labels. Chemistry and Physics of Lipids 111, 93–104.

Benatti, C.R., Lamy, M.T., Epand, R.M., 2008. Cationic amphiphiles and the solubilization of cholesterol crystallites in membrane bilayers. Biochimica et Biophysica Acta 1778, 844–853.

Blume, A., 1991. Phase transition of polymerizable phospholipids. Chemistry and Physics of Lipids 57, 253–273.

Campbell, R.B., Balasubramanian, S.V., Straubinger, R.M., 2001a. Influence of cationic lipids on the stability and membrane properties of paclitaxel-containing liposomes. Journal of Pharmaceutical Sciences 90 (8), 1091–1105.

Campbell, R.B., Balasubramanian, S.V., Straubinger, R.M., 2001b. Phospholipid-cationic lipid interactions: influences on membrane and vesicle properties. Biochimica et Biophysica Acta 1512, 27–39.

Clark, M.A., Blair, H., Liang, L., Brey, R.N., Brayden, D., Hirst, B.H., 2001. Targeting polymerised liposome vaccine carriers to intestinal M cells. Vaccine 20, 208–217.

Daly, S.M., Heffernan, L.A., Barger, W.R., Shenoy, D.K., 2006. Photopolymerization of mixed monolayers and black lipid membranes containing gramicidin A and diacetylenic phospholipids. Langmuir 22, 1215–1222.

Elouahabi, A., Ruysschaert, J.-M., 2005. Formation and intracellular trafficking of lipoplexes and polyplexes. Molecular Therapy 11 (3), 336–347.

Fabani, M.M., Gargini, R.A., Taira, M.C., Iacono, R., Alonso-Romanowski, S., 2002. Study of in vitro stability of liposomes and in vivo antibody response to antigen associated with liposomes containing GM1 after oral and subcutaneous immunization. Journal of Liposome Research 12, 13–27.

Felnerova, D., Viret, J.F., Glück, R., Moser, C., 2004. Liposomes and virosomes as delivery systems for antigens, nucleic acids and drugs. Current Opinion in Biotechnology 15, 518–529.

Freed, J.H., Fraenkel, G.K., 1963. Theory of line with in electron spin resonance spectra. Journal of Chemical Physics 39, 326–348.

Freeman, F.J., Hayward, J.A., Chapman, D., 1987. Permeability studies on liposomes formed from polymerisable diacetylenic phospholipids and their potential applications as drug delivery systems. Biochimica et Biophysica Acta 924, 341–351.

Gadras, C., Santaella, C., Vierling, P., 1999. Improved stability of highly fluorinated phospholipid-based vesicles in the presence of bile salts. Journal of Controlled Release 57, 29–34.

Gregoriadis, G., 1995. Engineering liposomes for drug delivery: progress and problems. Trends in Biotechnology 13, 527–537.

Griffith, O.H., Jost, P.C., 1976. Lipid spin labels in biological membranes. In: Berliner, L.J. (Ed.), Spin Labeling. Theory and Applications. Academic Press, New York, pp. 453–523.

Guo, C., Liu, S., Dai, Z., Jiang, C., Li, W., 2010. Polydiacetylene vesicles as a novel drug sustained-release system. Colloids and Surfaces B: Biointerfaces 76, 362–365.

Halpern, H.J., Peric, M., Yu, C., Bales, B.L., 1993. Rapid evaluation of parameters from inhomogeneously broadened EPR spectra. Journal of Magnetic Resonance 103, 13–22.

Hayward, J.A., Johnston, D.S., Chapman, D., 1985. Polymeric phospholipids as new biomaterials. Annals of the New York Academy of Sciences 446, 267–281.

Heimburg, T., 2000. A model for the lipid pretransition: coupling of ripple formation with the chain-melting transition. Biophysical Journal 78, 1154–1165.

Hubbell, W.L., McConnell, H.M., 1971. Molecular motion in spin-labeled phospholipids and membranes. Journal of the American Chemical Society 93, 314–326.

Ishiwata, H., Suzuki, N., Ando, S., Kikuchi, H., Kitagawa, T., 2000. Characteristics and biodistribution of cationic liposomes and their DNA complexes. Journal of Controlled Release 69, 139–148.

Jost, P.C., Griffith, O.H., 1976. Instrumental aspects of spin labeling. In: Berliner, L.J. (Ed.), Spin Labeling. Theory and Applications. Academic Press, New York, pp. 251–272.

Kshirsagar, N.A., Pandya, S.K., Kirodian, G.B., Sanath, S., 2005. Liposomal drug delivery system from laboratory to clinic. Journal of Postgraduate Medicine 51, 5–15.

Lundahl, P., Beigi, F., 1997. Immobilized liposome chromatography of drugs for model analysis of drug-membrane interactions. Advanced Drug Delivery Reviews 23, 221–227.

Markowitz, M.A., Chow, G.-M., Singh, A., 1994. Polymerized phospholipid membrane mediated synthesis of metal nanoparticles. Langmuir 10, 4095–4102.

Marsh, D., 1990. CRC Handbook of Lipid Bilayers. CRC press, Boston.

Mel'nikova, Y.S., Mel'nikov, S.M., Löfroth, J.-E., 1999. Physico-chemical aspects of the interaction between DNA and oppositely charged mixed liposomes. Biophysical Chemistry 81, 125–141.

Mohammed, A.R., Weston, N., Coombes, A.G.A., Fitzgerald, M., Perrie, Y., 2004. Liposome formulation of poorly water soluble drugs: optimisation of drug loading and ESEM analysis of stability. International Journal of Pharmaceutics 285, 23–34.

Morigaki, K., Schönherr, H., Okazaki, T., 2007. Polymerization of diacetylene phospholipid bilayers on solid substrate: influence of the film deposition temperature. Langmuir 23, 12254–12260.

Moses, M.A., Brem, H., Langer, R., 2003. Advancing the field of drug delivery: taking aim at cancer. Cancer Cell 4, 337–341.

Mozafari, M.R., 2005. Liposomes: an overview of manufacturing techniques. Cellular and Molecular Biology Letters 10, 711–719.

Noble, C.O., Guo1, Z., Hayes, M.E., Marks, J.D., Park, J.W., Benz, C.C., Kirpotin, D.B., Drummond, D.C., 2009. Characterization of highly stable liposomal and immunoliposomal formulations of vincristine and vinblastine. Cancer Chemotherapy and Pharmacology 64, 741–751.

Poste, G., Kirsh, R., Koestler, T., 1984. The challenge of liposome targeting in vivo. In: Gregoriadis, G. (Ed.), Liposome Technology, vol. 3. CRC Press, Boca Raton, pp. 1–28.

Pouton, C.W., Seymour, L.W., 2001. Key issues in non-viral gene delivery. Advanced Drug Delivery Reviews 46, 187–203.

Rao, N.M., 2010. Cationic lipid-mediated nucleic acid delivery: beyond being cationic. Chemistry and Physics of Lipids 163, 245–252.

Rawat, M., Singh, D., Saraf, S., Saraf, S., 2008. Lipid carriers: a versatile delivery vehicle for proteins and peptides. Journal of the Pharmaceutical Society of Japan 128, 269–280.

Riaz, M., 1995. Stability and uses of liposomes. Pakistan Journal of Pharmaceutical Sciences 8, 69–79.

Riske, K.A., Barroso, R.P., Vequi-Suplicy, C.C., Germano, R., Henriques, V.B., Lamy, M.T., 2009. Lipid bilayer pre-transition as the beginning of the melting process. Biochimica et Biophysica Acta 1788, 954–963.

Samad, A., Sultana, Y., Aqil, M., 2007. Liposomal drug delivery systems: an update review. Current Drug Delivery 4, 297–305.

Schreier, S., Polnaszek, C.F., Smith, I.C., 1978. Spin labels in membranes. Problems in practice. Biochimica et Biophysica Acta 515, 395–436.

Sharma, A., Sharma, U.S., 1997. Liposomes in drug delivery: progress and limitations. International Journal of Pharmaceutics 154, 123–140.

Subramaniam, V., Dĭ Ambruoso, G.D., Hall Jr., H.K., Wysocki Jr., R.J., Brown, M.F., Saavedra, S., 2008. Reconstitution of rhodopsin into polymerizable planar supported lipid bilayers: influence of dienoyl monomer structure on photoactivation. Langmuir 24, 11067–11075.

Svenson, S., Messersmith, P.B., 1999. Formation of polymerizable phospholipid nanotubules and their transformation into a network gel. Langmuir 15, 4464–4471.

Takeuchi, H., Yamamoto, H., Toyoda, T., Toyobuku, H., Hino, T., Kawashima, Y., 1998. Physical stability of size controlled small unilameller liposomes coated with a modified polyvinyl alcohol. International Journal of Pharmaceutics 164, 103–111.

Temprana, C.F., Amor, M.S., Femia, A.L., Gasparri, J., Taira, M.C., Alonso, S., del, V., 2011. Ultraviolet irradiation of diacetylenic liposomes as a strategy to improve

size stability and to alter protein binding without cytotoxicity enhancement. Journal of Liposome Research 21 (2), 141–150.
Temprana, C.F., Duarte, E.L., Taira, M.C., Lamy, M.T., Alonso, S., del, V., 2010. Structural characterization of photopolymerizable binary liposomes containing diacetylenic and saturated phospholipids. Langmuir 26 (12), 10084–10092.
Temprana, C.F., 2011. Diseño y caracterización de polímeros lipídicos como posibles vectores para transfección, 2011. PhD Thesis. Universidad Nacional de Quilmes, Bernal, Argentina.
Tros de Ilarduya, C., Sun, Y., Düzgüneş, N., 2010. Gene delivery by lipoplexes and polyplexes. European Journal of Pharmaceutical Sciences 40, 159–170.
Ulrich, A.S., 2002. Biophysical aspects of using liposomes as delivery vehicles. Bioscience Reports 22 (2), 129–150.
Zhang, Y., Garzon-Rodriguez, W., Manning, M.C., Anchordoquy, T.J., 2003. The use of fluorescence resonance energy transfer to monitor dynamic changes of lipid–DNA interactions during lipoplex formation. Biochimica et Biophysica Acta 1614, 182–192.